Detailed Studies of the Nuclear Dependence of $R = \sigma_L/\sigma_T$

J. Arrington

Argonne National Laboratory, Argonne, IL 60439, USA

V. Mamyan

Carnegie Mellon University, Pittsburgh, PA 15213, USA

S. P. Malace

Duke University, Durham, NC 27708, USA

P. E. C. Markowitz

Florida International University, Miami, FL 33199, USA

A. Accardi, M. E. Christy(spokesperson), J. Diefenbach, Y. Han, C. E. Keppel(spokesperson), M. Kohl, P. Monaghan, L. Tang, and L. Y. Zhu(spokesperson)

Hampton University, Hampton, VA 23668, USA

G. Niculescu and I. Niculescu

James Madison University, Harrisonburg, VA 22807, USA

B. T. Hu

Lanzhou University, Lanzhou, Gansu Province, China

X. Jiang and A. Puckett

Los Alamos National Laboratory, Los Alamos, NM 87544, USA

V. Sulkosky

Massachusetts Institute of Technology, Cambridge, MA 02139, USA

J. Dunne, D. Dutta

Mississippi State University, Mississippi State, MS 39762, USA

R. Ent, H. Fenker, D. Gaskell(spokesperson), V. Guzey, M. Jones, B. Sawatzky, P. Solvignon(spokesperson), and S. Wood

Thomas Jefferson National Accelerator Facility, Newport News, VA 23606, USA

A. Daniel

Ohio University, Athens, OH 45701, USA

A. Atkins, T. Badman, J. Maxwell, S. Phillips, K. Slifer, and R. Zielinski

University of New Hampshire, Durham, NH 03824, USA

G. Huber

University of Regina, Regina, SK S4S0A2, Canada.

A. Bodek

University of Rochester, Rochester, NY 14627, USA.

H. Baghdasaryan, D. Day, N. Kalantarians, and M. Yurov

University of Virginia, Charlottesville, VA 22904, USA

A. Asaturyan, A. Mkrtchyan, H. Mkrtchyan, V. Tadevosyan, and S. Zhamkochyan

Yerevan Physics Institute, 2 Alikhanyan Brothers St., Yerevan 0036, Armenia

(Dated: July 5, 2011)

Abstract

We propose to measure inclusive inelastic electron-nucleon and electron-nucleus scattering cross sections spanning the four-momentum transfer range $0.4 < Q^2 < 6$ GeV^2 using hydrogen, deuterium, carbon, copper, tin, and gold targets. The cross sections will be used to perform Rosenbluth-type separations to extract the ratio $R = \sigma_L/\sigma_T$, and to separate the transverse, longitudinal, and mixed structure functions (F_1, F_L, and F_2) model-independently. The ratio R has been reasonably well measured in deep inelastic scattering over a wide range of kinematics using hydrogen and deuterium targets, however very few measurements exist on nuclei.

The ratio of the structure function F_2 measured in nuclei as compared to deuterium demonstrated that nucleons inside a nucleus may have a different distribution of momentum among their component quarks than in a nucleon. While it is now possible to identify some of the necessary ingredients in an explanation of the nuclear dependence of the structure function, there are still competing models that lead to significantly different pictures of this "EMC effect" and this phenomenon remains an active area of study.

Experimentally, the extraction of the F_2 ratios from the measured inclusive cross section ratios is not straightforward if there is non-trivial nuclear dependence on $R = \sigma_L/\sigma_T$, i.e. $R_A - R_D \neq 0$. The JLab E99-118 data suggest R may be slightly different between hydrogen and deuterium targets at $Q^2 < 1$ GeV^2, which might be more pronounced between heavy nuclear targets and deuterium. The SLAC E140 data suggest that R may be slightly different between iron and deuterium at $x = 0.2$. A recent re-analysis of SLAC and JLab E03-103 data at large x suggest that the nuclear dependence of R is no longer trivial in the EMC region if Coulomb corrections are included – an observation that could potentially change the interpretation of the EMC effect. This proposal will broaden the measured longitudinal-transverse structure function kinematics, and study the nuclear dependence of R at smaller x where R is bigger but the EMC effect is smaller. We propose in particular a wide kinematics region to disentangle the x dependence and Q^2 dependence, to study the nuclear dependence of R in a systematic way. We also propose to take supplementary data to check the current estimates of Coulomb corrections and (quasi-)elastic radiative corrections.

Moreover, improved understanding of nuclear modifications to the structure functions should assist nuclear parton distribution studies as well as testing of theoretical models of nuclear modifications to structure functions. The longitudinal structure function F_L may provide important information in this regard, allowing unique sensitivity to gluon distributions.

Contents

1. Introduction 4

2. Formalism 9

3. Physics Motivations and Proposed Measurements 11

3.1. Nuclear Dependence of R 11

3.2. Q^2 Dependence of R 15

3.3. Some Discussions on F_L 17

4. Experiment 20

4.1. Experimental Overview 20

4.2. Systematic Uncertainty 21

4.3. Beam Time Request 22

5. Summary 24

6. Commitment to the Hall C 12 GeV upgrade 24

A. Event Rates 25

B. Studies of Systematic Uncertainties 26

1. Radiative Corrections 26

2. Coulomb Correction 26

3. Charge Symmetric Background 26

4. π^-/e Ratio 32

References 32

1. INTRODUCTION

Since the early lepton scattering experiments discovered the substructure of the nucleon and led to the development of the quark-parton model, deep-inelastic-scattering (DIS) has proved to be a critical tool in the investigation of nucleon and nuclear structure. The nucleon structure function F_2 has been measured to high precision in x and Q^2. The longitudinal

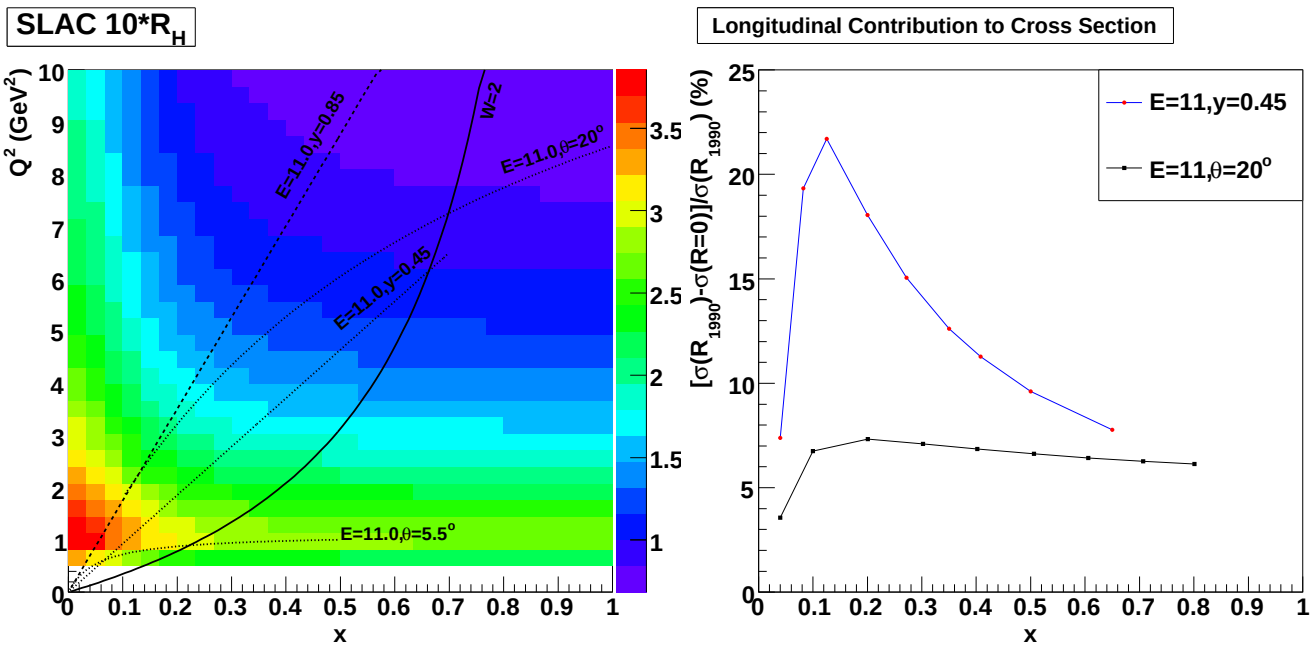

FIG. 1: [Left] The magnitude of R (scaled by a factor of 10) for a hydrogen target based on the SLAC R_{1990} fit as a function of x and Q^2. [Right] The percentage of the longitudinal contribution to the total inclusive cross section based on the SLAC R_{1990} fit.

structure function F_L, in contrast, is not as well measured and data are lacking in particular for nuclear targets. It is necessary to separate the longitudinal and transverse structure functions in order to precisely measure them, especially at lower values of Q^2 and x. This may be accomplished via measurements of the longitudinal to transverse cross section ratio, $R = \sigma_L/\sigma_T$. The longitudinal to transverse ratio $R = \sigma_L/\sigma_T$ for the proton is plotted in Figure 1 based on the R_{1990} fit from Whitlow's re-analysis of the SLAC data [1]. R ranges from 0.07 to 0.39 in the plotted $Q^2 < 10$ GeV^2 region. As two examples with 11 GeV beam, the longitudinal contribution can be up to 22% for a fixed-momentum measurement at $E' = 6.1$ GeV (or $y = 0.45$), and is around 7% for a fixed-angle measurement at 20 degrees. It will be necessary to measure R for precision determinations of the inclusive structure functions for the JLab 12 GeV upgrade.

JLab Hall C has had a successful 6 GeV program [2–7] to measure the longitudinal/transverse (L/T) separated structure functions, using the Rosenbluth technique [8]. This program has significantly expanded the global data sets of structure functions on the nucleon and nuclei. But, due to the beam energy constraint, most data are in the resonance

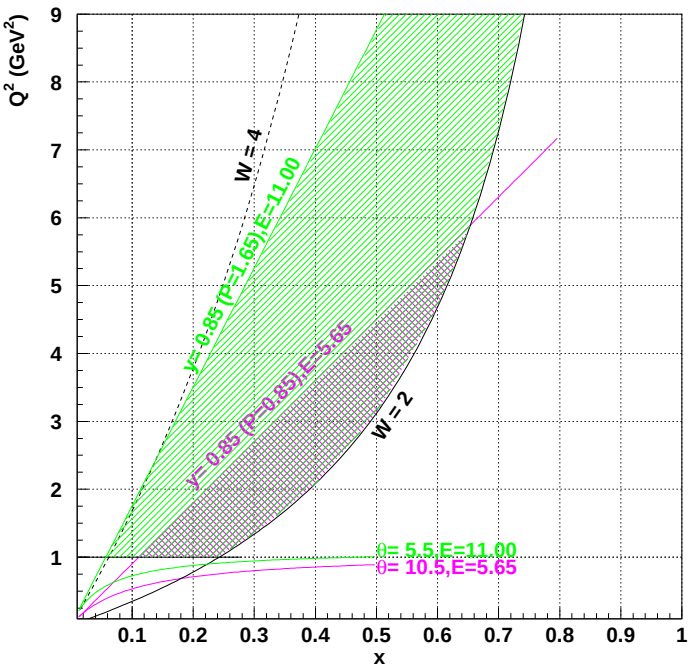

FIG. 2: The expansion of the DIS kinematics coverage by upgrading the 5.65 GeV electron beam (red shaded area) to 11 GeV (green shaded area). The upper boundary is defined by the $y = 0.85$ line. Larger y region generally involves significant experimental challenges, in particular large radiative corrections. The lower boundaries are defined by the $Q^2 > 1$ GeV^2 and $W > 2$ GeV curves. If including the resonance contribution, the kinematics coverage may extend to the curve corresponding to the most forward angle of the spectrometer (10.5^o for HMS and 5.5^o for SHMS).

region. The magenta shaded area in Figure 2 shows the DIS kinematic region that can be accessed by the 5.65 GeV beam. The L/T separated DIS region is even smaller since the Rosenbluth technique requires a sizable beam energy span. The proposed R experiment in Hall C after the 12 GeV upgrade is a natural extension of the existing Rosenbluth program at 6 GeV, allowing wider coverage in the DIS region. For the overlapping kinematic region, the expansion of the maximum beam energy to 11 GeV will increase the ϵ coverage and greatly reduce the statistical and systematic uncertainties in the Rosenbluth-separated R measurements.

We propose to measure the nuclear dependence of R for several different targets (H, D, C, Al, Cu, Sn, Au) over a broad kinematic region: $0.4 < Q^2 < 6$ GeV^2 and $0.04 < x <$

0.65. These measurements may have a profound impact on the understanding of nuclear modifications to the inclusive cross sections and F_2 structure functions, for example the EMC effect in $0.3 < x < 0.7$ region. Since its original observation [14], the EMC effect has inspired intense experimental and theoretical study (see Refs. [15, 16] for recent reviews). A non-zero value of $R_A - R_D$ has two potential effects on our understanding of the origin of the EMC effect. First, $R_A - R_D \neq 0$ must be explained by any model that attempts to describe the EMC effect. For example, a model that includes additional spin-0 constituents in nuclei, like "nuclear pions" for example, might naturally lead to some modification of R. Second, at a more practical level, measurements of the EMC effect typically assume $R_A - R_D = 0$ (or at least very small) such that measurements of *unseparated* cross section ratios between nuclei and deuterium are equivalent to measuring the ratio of F_2 structure functions, i.e., $\frac{\sigma_A}{\sigma_D} = \frac{F_2^A}{F_2^D}$. In the case, $R_A \neq R_D$, our simple interpretation of the cross section ratio directly representing the modification of quark distributions is thrown into question.

This latter point is illustrated in Fig. 3. The plot on the left shows the (isoscalar corrected) inclusive cross section ratio for iron and copper as measured by the SLAC 139 [17] and EMC [18] collaborations. In the assumption that $R_A = R_D$, the cross sections ratios correspond directly to the modification of the F_2 structure functions. However, there are some hints of a non-trivial nuclear dependence of R. The JLab E99-118 data suggest R may be slightly different between hydrogen and deuterium targets at $Q^2 < 1$ GeV^2 [3]. The SLAC E140 data suggest that R may be slightly different between iron and deuterium at $x = 0.2$ [10]. In addition, a recent re-analysis [9] of SLAC E140 [10] and JLab E03-103 [11] data suggest that the nuclear dependence of R may not be trivially small in the EMC region ($0.3 < x < 0.7$) if Coulomb corrections are included. The potential effect of this difference is illustrated by the plot on the right in Fig. 3. In this plot, a re-analysis of the world's data was performed, examining the nuclear dependence of σ_A/σ_D at fixed ϵ to extract the effective ratio for nuclear matter. This was performed for several values of ϵ such that one could then extract the ratio in the $\epsilon = 0$ limit, i.e., F_1^A/F_1^D. The result of this extraction is shown by the solid red circles. The impact is dramatic - the size of the nuclear modification is greatly suppressed in the large x region. However, this extraction is hindered by the fact that one is forced to perform this analysis on the world's data, combining data taken at low ϵ from one experiment with data at larger ϵ from other experiments. It is crucial that a single, systematically controlled experiment be used to aid in this analysis.

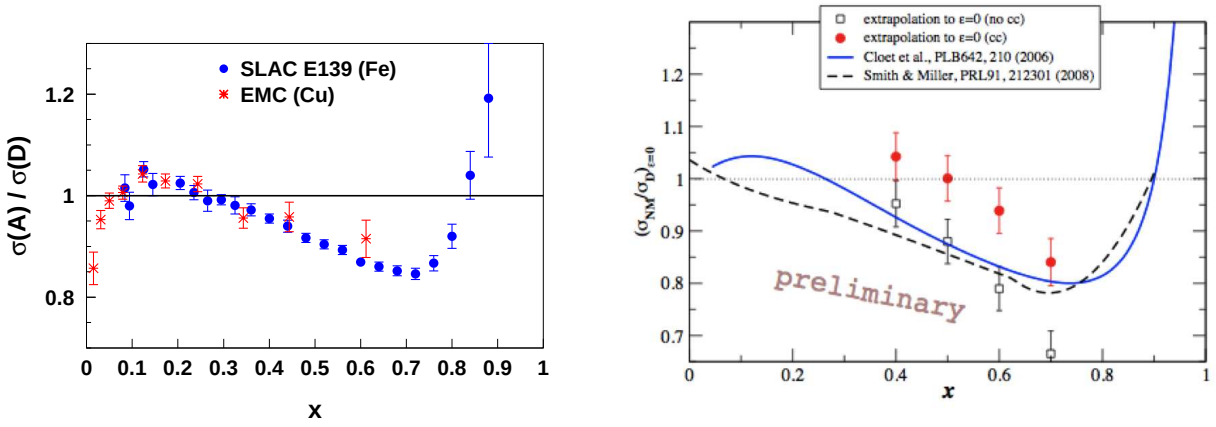

FIG. 3: [Left] Inclusive cross section ratio for iron and copper as measured by the SLAC 139 [17] and EMC [18] collaborations. [Right] F_1^A/F_1^D for nuclear matter with (red solid circles) and without (black open circles) Coulomb corrections. The F_1 structure function ratio is determined by: 1) extrapolating cross section ratios at fixed values of ϵ to nuclear matter and 2) fitting the nuclear matter ratio vs. $\epsilon' = \epsilon/(1+\epsilon R_D)$. The nuclear matter F_1 ratio is the value at $\epsilon' = 0$.

It is also important to point out that the analysis in Fig. 3 (right) incorporates the use of so-called "Coulomb corrections". At large x in particular, the estimated effects from Coulomb acceleration (deceleration) in the field of the Z protons of a heavy nucleus can be sizable, approaching 5-10%. They have typically been estimated based on the (modified) Effective Momentum Approximation (EMA), which has been rigorously tested for quasi-elastic scattering [12, 13].

Due to their significant impacts on the extraction of R in nuclear targets, we will also take some data to check the current estimations of Coulomb corrections. The EMA technique for Coulomb corrections has not been tested for deep-inelastic scattering. We propose to measure the cross section ratio σ_A/σ_D, at fixed ϵ for a range of Q^2. This exercise will sample a range of initial and scattered electron momenta, hence changing the magnitude of the Coulomb corrections. Under the assumption that the EMC Effect (and $R_A - R_D$ if it is non-zero) is Q^2 independent, the target ratio should be constant, allowing us to test the EMA, or any other Coulomb correction technique that will have been developed by the time this experiment runs.

The proposed R measurements will also used to study the Q^2 dependence of R at fixed electron momentum. R is supposed to vanish at the real photon limit at fixed electron

momentum (or ν), but this behavior has not yet been tested. In addition, the proposed R measurements will expand the Hall C F_L measurements at $Q^2 = 0.75, 1.75, 2.5, 3.75$ GeV^2. The F_L structure functions is uniquely sensitive to the gluon distributions, and few measurements exist for the nuclear targets.

2. FORMALISM

Due to the small value of the electromagnetic coupling constant, the scattering of electrons from nucleons can be well approximated by the exchange of a single virtual photon. In terms of the incident electron energy E, the scattered electron energy $E^{'}$, and the scattering angle θ, the absolute value of the exchanged 4-momentum squared Q^2 is given by

$$Q^2 = -q^2 = 4EE^{'}\sin^2\frac{\theta}{2} \ . \tag{1}$$

In this one photon exchange approximation, the spin-independent cross section for inclusive electron-nucleon scattering can be expressed in terms of the photon helicity coupling as

$$\frac{d^2\sigma}{d\Omega dE'} = \Gamma\left[\sigma_T(x,Q^2) + \epsilon\sigma_L(x,Q^2)\right] = \Gamma\sigma_T(x,Q^2)\left[1 + \epsilon R(x,Q^2)\right] \ , \tag{2}$$

where σ_T (σ_L) is the cross section for photo-absorption of purely transverse (longitudinal) polarized photons. Bjorken x is the fraction of the momentum carried by the quarks and gluons inside the nucleon and can be expressed as $x = \frac{Q^2}{2M(E-E^{'})}$ in the lab frame with nucleon mass M.

$$\Gamma = \frac{\alpha E^{'}(W^2 - M^2)}{4\pi^2 Q^2 M E(1-\epsilon)} \tag{3}$$

is the flux of transverse virtual photons expressed in terms of the strong coupling constant α, the invariant mass W, the energy transfer $\nu = E - E^{'}$, and the virtual photon polarization parameter

$$\epsilon = \left[1 + 2(1 + \frac{\nu^2}{Q^2})\tan^2\frac{\theta}{2}\right]^{-1} \ . \tag{4}$$

Note $\epsilon = 0$ for purely transverse polarization. It can be also expressed in terms of $y = \nu/E$ and Q^2/E^2

$$\epsilon = \frac{4(1-y) - \frac{Q^2}{E^2}}{4(1-y) + 2y^2 + \frac{Q^2}{E^2}} \ . \tag{5}$$

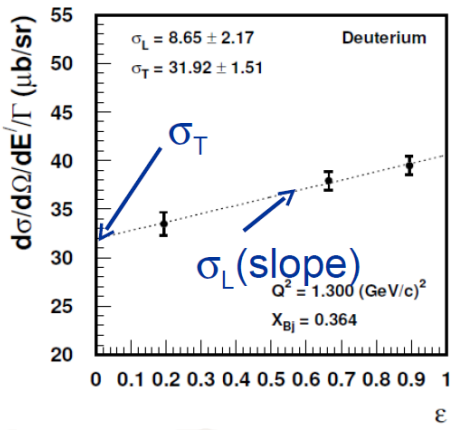

FIG. 4: An example L/T separation using the Rosenbluth technique.

At small Q^2 ($<< E^2$), ϵ only depends on y, with the relation $\epsilon = 1 - \frac{y^2}{1+(1-y)^2}$. This implies that $\epsilon = 1$ at $y = 0$, and $\epsilon = 0$ at $y = 1$. The study of the ϵ dependence at JLab, is therefore complementary to the recent studies of the $\frac{y^2}{1+(1-y)^2}$ dependence at H1 and ZEUS.

In terms of the structure functions $F_1(x, Q^2)$ and $F_2(x, Q^2)$ in the DIS region, the double differential cross section can be written as

$$\frac{d^2\sigma}{d\Omega dE'} = \Gamma \frac{4\pi^2\alpha}{x(W^2 - M^2)} \left[2xF_1(x, Q^2) + \epsilon \left((1 + \frac{4M^2x^2}{Q^2})F_2(x, Q^2) - 2xF_1(x, Q^2) \right) \right]. \quad (6)$$

A comparison of Equation 2 and Equation 6 shows that $F_1(x, Q^2)$ is purely transverse, while the combination

$$F_L(x, Q^2) = (1 + \frac{4M^2x^2}{Q^2})F_2(x, Q^2) - 2xF_1(x, Q^2) \quad (7)$$

is purely longitudinal.

The separation of the unpolarized structure functions into longitudinal and transverse parts from cross section measurements can be accomplished via the Rosenbluth technique [8], by making measurements at two or more ϵ points at fixed x and Q^2. Fitting the reduced cross section, $d\sigma/\Gamma$, linearly in ϵ, yields σ_T (and therefore $2xF_1(x, Q^2)$) as the intercept, and σ_L (and therefore $F_L(x, Q^2)$) as the slope. The longitudinal to transverse cross section ratio $R(x, Q^2) = \sigma_L/\sigma_T = F_L(x, Q^2)/2xF_1(x, Q^2)$ can then be obtained. An example of this approach is shown in Figure 4.

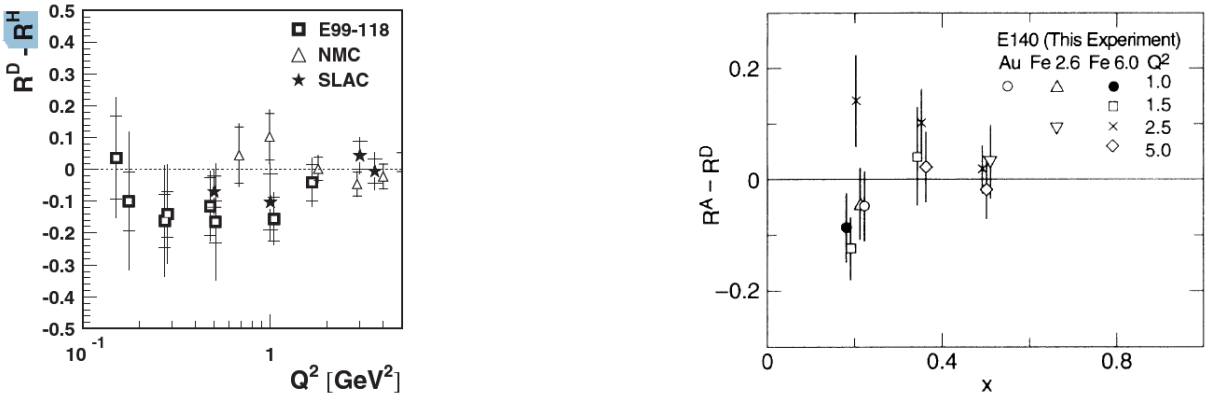

FIG. 5: [left] [3] The difference between R_D and R_H as a function of Q^2 from the JLab E99-118 experiment, as well as previous SLAC data. [right] [10] The difference between R_{Fe}/R_{Au} and R_D from the SLAC E140 experiment, as a function of Bjorken x and for different Q^2 bins.

3. PHYSICS MOTIVATIONS AND PROPOSED MEASUREMENTS

3.1. Nuclear Dependence of R

A precision R measurement is necessary to have a model independent determination of the structure functions, including F_2. It is very important for the global parameterizations of the Parton Distribution Functions (PDFs) and its nuclear modifications. There are several areas where existing data hints a non-trivial nuclear dependence of R.

The nuclear dependence of $R = \sigma_L/\sigma_T$ in DIS was measured by the HERMES collaboration [22] via fitting the cross section ratio σ_A/σ_D as a function of virtual photon polarization ϵ over a typical range of $0.4 < \epsilon < 0.7$. Overall no significant ϵ-dependence was observed for $\sigma_{^{14}N}/\sigma_D$ and $\sigma_{^3He}/\sigma_D$. However, at low x ($0.01 < x < 0.03$), R_A/R_D seems to be greater than 1. Since the ϵ-dependence at HERMES may be coupled with Q^2-dependence due to a single beam energy, it is essential to improve the precision of the HERMES measurement in the low x region with real Rosenbluth separations.

At small Q^2, a sizable difference in R was observed between deuterium and hydrogen targets in the JLab E99-118 experiment, shown as $R_D - R_H$ in Figure 5 [3]. The preliminary data from JLab E00-002 experiment also indicate negative $R_D - R_H$ in this kinematic range [4]. A precise comparison of R between heavy targets and deuterium target, $R_A - R_D$, is helpful to understand the difference of R between hydrogen and deuterium.

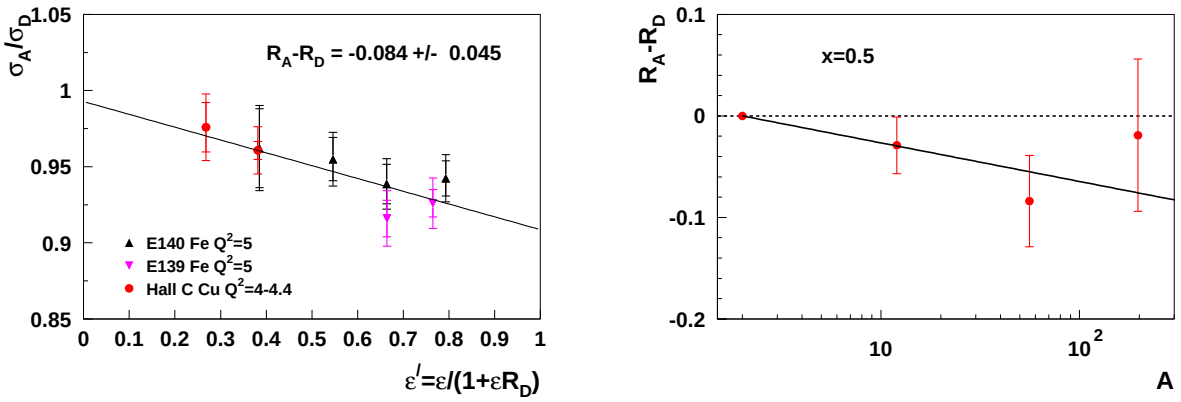

FIG. 6: Combined analysis of data from SLAC E139, E140,and Hall C experiment E03-103 at $x = 0.5$, $Q^2 \approx 5$ GeV^2. The plot on the left shows the $\epsilon'(= \epsilon/(1 + \epsilon R_D)$ dependence of σ_A/σ_D for Cu and Fe targets, while the plot on the right shows the extracted value of $R_A - R_D$ for carbon, copper/iron, and gold at the same kinematics [9].

At $x = 0.2$, the SLAC E140 data [10] seem to suggest some nuclear dependence of R, which may have non-trivial Q^2 dependence, as shown in Figure 5. $R_{Fe} - R_D$ can be positive at $Q^2 = 2.5$ GeV^2 and negative at $Q^2 = 1.5$ GeV^2. It is not clear whether this few σ deviation is due to statistical fluctuations.

At larger x in the EMC region, the SLAC E140 experiment found no evidence for a nuclear dependence of R. However, re-analysis of that data set including Coulomb corrections (which had not been included previously) suggests a non-zero value for $R_A - R_D$. In particular, when combined with preliminary results from JLab experiment E03-103, the deviation from zero is almost 2 σ at $x = 0.5$ [9], as shown in Fig. 6. In this analysis, measurements of σ_A/σ_D at low ϵ from Hall C experiment E03-103 were combined with measurements from SLAC experiments E139 and E140 at $Q^2 \approx 5$ GeV^2. Care was taken to appropriately incorporate the normalization errors from the different data sets in the point-to-point uncertainties, although one had to make the mild assumption that it was appropriate to combine data from copper at $Q^2 = 4.4$ GeV^2 (Hall C) with data at $Q^2 = 5$ GeV^2 from iron. With these caveats, though, the non-zero value of $R_A - R_D$ is still very interesting, and if confirmed, has important ramifications for our understanding of the origin of the EMC effect discussed in Section 1. Further analysis was performed on carbon and gold targets to attempt to extract the effective A dependence of the effect, also shown in Fig. 6.

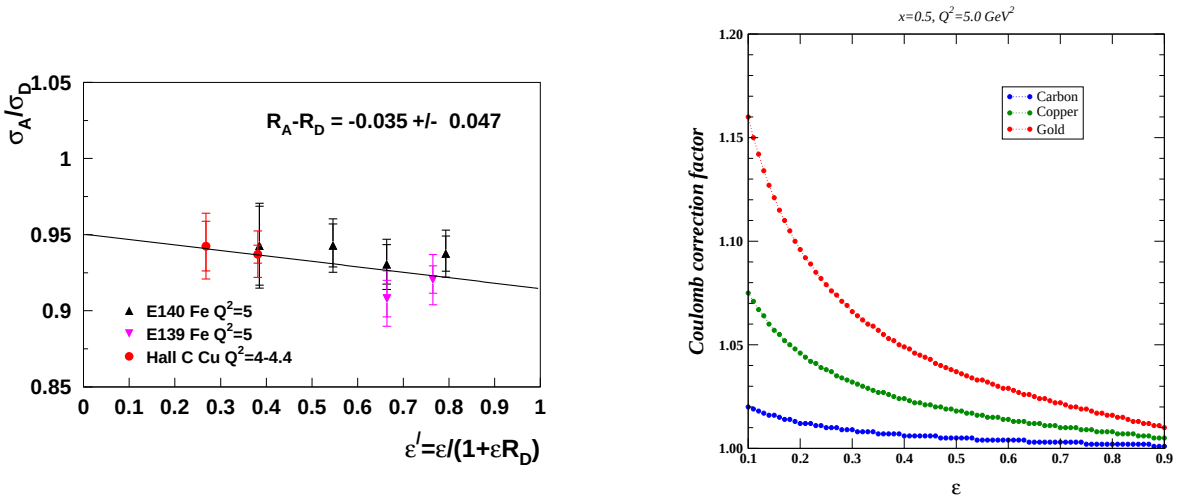

FIG. 7: The SLAC/Hall C combined analysis (see Fig. 6) at x=0.5, Q^2=5 GeV^2 with no Coulomb corrections (left). Without Coulomb corrections, the extracted value of $R_A - R_D$ is consistent with zero. The plot on the right shows the size of the predicted Coulomb corrections for Carbon, Copper, and Gold plotted vs. ϵ. The ϵ dependence of the effect makes it clear that understanding these corrections is crucial to Rosenbluth separations involving nuclear targets.

It is worth commenting at this point that a key ingredient in the non-zero value of $R_A - R_D$ extracted from the above analysis is the Coulomb correction procedure. Indeed, if the same Coulomb correction procedure had been applied to the E140 data alone, the extracted value at x=0.5, Q^2=5 GeV^2 would have been $R_A - R_D = -0.051 \pm 0.056$, a change of almost 1 σ from the original result. In Fig. 7, the same Hall C/SLAC combined analysis is shown with no Coulomb corrections applied. In this case, the slope is completely consistent with zero, and a fit of the ϵ dependence of the target ratios to a constant yields a reasonable χ^2. The size of the Coulomb corrections for various nuclei at x=0.5, Q^2=5 GeV^2 is also illustrated in Fig. 7. The ϵ dependence of the Coulomb correction makes it obvious that these effects must be under control for any attempt to perform a Rosenbluth separation using nuclear targets to be successful.

This sensitivity to the Coulomb corrections has motivated us to try verifying the prescription experimentally. Ideally, this would be done by comparing data from electron and positron beams. Unfortunately, we have no easy access to positrons, so another method must be explored. In this experiment, we propose to measure target cross section ratios at fixed ϵ to vary the size of the Coulomb corrections with the expectation that the target ratio should remain constant.

The unseparated cross section ratio can be written,

$$\frac{\sigma_A}{\sigma_D} = \frac{\sigma_A^T}{\sigma_D^T}\left[1 + \frac{\epsilon}{1+\epsilon R_D}(R_A - R_D)\right]. \quad (8)$$

At fixed ϵ, one is primarily sensitive to σ_A^T/σ_D^T; ϵR_D is small and one makes the assumption that $R_A - R_D$ does not vary quickly with Q^2. Since the EMC effect as studied at large ϵ has been demonstrated to be Q^2 independent to a large degree, one can vary E and E' (and hence Q^2), changing the magnitude of the Coulomb correction, yet the unseparated target ratio is expected to remain constant.

We propose to perform such a study at $x = 0.5$, varying Q^2 from 3.5 to 9.0 GeV^2 at $\epsilon = 0.2$. Over this range, the predicted Coulomb correction factor will change by about 5%. We also propose to take data at $\epsilon = 0.7$ for Q^2=2.1 and 5.8 GeV^2; here the variation of the expected Coulomb correction factor should be much smaller, 1.5%. This will help provide a systematic check that we are indeed not terribly sensitive to the Q^2 variation at fixed ϵ. The kinematics for this study are shown in Table VIII.

In this experiment, we will extract $R_A - R_D$ with the Rosenbluth technique, i.e. linear fitting the A/D cross section ratios at different ϵ settings. At small R, Equation 8 can be further simplified and $R_A - R_D$ is directly related to a double cross section ratio:

$$R_A - R_D \approx \frac{1 - \frac{d\sigma_{1A}}{d\sigma_{1D}} \cdot \frac{d\sigma_{2D}}{d\sigma_{2A}}}{\epsilon_2 - \epsilon_1} \quad (9)$$

The proposed production kinematics are summarized in Figure 8, as well as Table I and Table II. The solid circles are the kinematics proposed for the measurement of R with all nuclear targets (H, D, C, Cu, Sn, Au), while the open circles and triangles are test kinematics with only three targets (D, C, Au). Aluminum "Dummy" targets will be used for all kinematics for the end-cap subtraction for the hydrogen and deuterium targets. The allowed kinematic region for each beam energy can be defined in Figure 8 as the region between the fixed y straight line at large Q^2 and most forward angle line at low Q^2. Generally speaking, kinematics with a larger y has wider ϵ span so that it is important to measure R with y as big as possible. However at large y, there may be large (quasi-)elastic radiative tail contributions. We have chosen our kinematics with $y < 0.75$ so that the (quasi-)elastic radiative corrections are under control. We have a few kinematics in open circles to check the (quasi-)elastic radiative corrections at larger y in order to minimize the systematic uncertainties. Fixed y means fixed momentum for the scattered electrons. Experimentally,

it is faster to adjust spectrometer angles than momenta. We have three lines of measurement along y$\sim$0.75 for 4.4, 6.6 and 8.8 GeV beam. The central kinematics along $y = 0.74$ for $E = 6.6$ GeV can be accessed by 6.6, 8.8 and 11.0 GeV beam except the lowest x/Q^2 two points due to the angle constraint. The upper kinematics along $y = 0.75$ for the $E = 8.8$ GeV can be only accessed by 8.8 and 11.0 GeV beam and the ϵ coverage is smaller than the central kinematics. The lower kinematics along $y = 0.75$ for the $E = 4.4$ GeV can be accessed from 4.4 to 11.0 GeV beam and the ϵ coverage is bigger than the central kinematics. The lower kinematics can be possibly measured with the Hall C 6 GeV program but the ϵ coverage is very limited there. The triangles show the proposed kinematics to check the model for Coulomb corrections.

The hatched area in the right panel of Figure 8 indicates the kinematic coverage of previous Hall C measurements of R with the 6 GeV beam for the following targets: H, D, C, Al, and Cu from E94-110 [2], E99-118 [3],E02-109 [5], E04-001 [6], and E06-009 [7]. The preliminary results from the deuterium and heavy targets are currently being finalized and the preliminary results point towards a moderate nuclear dependence of R. The overlap in the proposed measurements and the existing measurements is critical for cross normalization of the proposed cross section measurements with the existing data sets.

The projection for R and $R_A - R_D$ is shown in Figure 10 where only the point-point systematic uncertainties matter. The relative uncertainty for the right plot is smaller due to bigger cancellation in the target ratios.

3.2. Q^2 Dependence of R

At $Q^2 \to 0$, the virtual photon will approach the real photon limit, where there is no longitudinal component and $R = 0$. Therefore one expects $R \to 0$ at the limit of $Q^2 \to 0$. This can be also derived from the general definition of the hadronic tensor:

$$W^{\mu\nu} = \frac{F_1}{M}\left(-g^{\mu\nu} + \frac{q^\mu q^\nu}{q^2}\right) + \frac{F_2}{M(p\cdot q)}\left(p^\mu - \frac{p\cdot q}{q^2}q^\mu\right)\left(p^\nu - \frac{p\cdot q}{q^2}q^\nu\right) \tag{10}$$

and it can be rearranged in the form

$$W^{\mu\nu} = -\frac{F_1}{M}g^{\mu\nu} + \frac{F_2}{M(p\cdot q)}p^\mu p^\nu + \left(\frac{F_1}{M} + \frac{F_2}{M}\frac{p\cdot q}{q^2}\right)\frac{q^\mu q^\nu}{q^2} - \frac{F_2}{M}\frac{p^\mu q^\nu + q^\mu p^\nu}{q^2} \tag{11}$$

To eliminate the potential kinematic singularities of $W^{\mu\nu}$ at $Q^2 \to 0$ requires that $F_2 = O(Q^2)$ and $\frac{F_1}{M} + \frac{F_2}{M}\frac{p\cdot q}{q^2} = O(Q^2)$. Therefore $F_L = (1+\frac{Q^2}{\nu^2})F_2 - 2xF_1 = O(Q^4)$ and $R = \frac{F_L}{2xF_1} =$

Q^2	x_b	E	E'	θ	ϵ	y	W
0.37	0.040	6.6	1.7	10.4	0.477	0.742	3.12
0.36	0.040	8.8	3.9	5.9	0.737	0.557	3.12
0.76	0.082	6.6	1.7	14.9	0.471	0.742	3.05
0.75	0.082	8.8	3.9	8.5	0.734	0.557	3.05
1.15	0.125	6.6	1.7	18.4	0.465	0.742	2.99
1.15	0.125	8.8	3.9	10.5	0.730	0.557	2.99
1.15	0.125	11.0	6.1	7.5	0.842	0.445	2.99
1.85	0.201	6.6	1.7	23.4	0.454	0.742	2.87
1.84	0.200	8.8	3.9	13.3	0.724	0.557	2.87
1.84	0.200	11.0	6.1	9.5	0.838	0.445	2.87
2.50	0.272	6.6	1.7	27.3	0.444	0.742	2.75
2.50	0.271	8.8	3.9	15.5	0.718	0.557	2.75
2.51	0.273	11.0	6.1	11.1	0.834	0.445	2.75
3.23	0.351	6.6	1.7	31.1	0.433	0.742	2.62
3.21	0.349	8.8	3.9	17.6	0.711	0.557	2.62
3.23	0.351	11.0	6.1	12.6	0.830	0.445	2.62
3.75	0.408	6.6	1.7	33.6	0.426	0.742	2.52
3.74	0.407	8.8	3.9	19.0	0.706	0.557	2.52
3.76	0.409	11.0	6.1	13.6	0.827	0.445	2.51
4.59	0.499	6.6	1.7	37.3	0.413	0.742	2.34
4.60	0.500	8.8	3.9	21.1	0.699	0.557	2.34
4.57	0.497	11.0	6.1	15.0	0.822	0.445	2.35
5.98	0.650	6.6	1.7	42.8	0.393	0.742	2.02
5.98	0.651	8.8	3.9	24.1	0.686	0.557	2.02
6.00	0.653	11.0	6.1	17.2	0.814	0.445	2.02

TABLE I: The central kinematics (along the line of $E = 6.6, y = 0.74$) to measure the nuclear dependence of R.

Q^2	x_b	E	E'	θ	ϵ	y	W
0.75	0.061	8.8	2.2	11.3	0.464	0.750	3.54
0.74	0.060	11.0	4.4	7.1	0.685	0.600	3.54
1.75	0.141	8.8	2.2	17.3	0.455	0.750	3.39
1.75	0.141	11.0	4.4	10.9	0.679	0.600	3.39
2.50	0.202	8.8	2.2	20.7	0.449	0.750	3.28
2.48	0.200	11.0	4.4	13.0	0.675	0.600	3.28
3.74	0.302	8.8	2.2	25.4	0.438	0.750	3.09
3.75	0.303	11.0	4.4	16.0	0.667	0.600	3.08
4.34	0.351	8.8	2.2	27.4	0.433	0.750	2.99
4.33	0.350	11.0	4.4	17.2	0.664	0.600	2.99
6.21	0.501	8.8	2.2	32.9	0.417	0.750	2.66
6.19	0.500	11.0	4.4	20.6	0.653	0.600	2.66
0.75	0.121	4.4	1.1	22.7	0.444	0.750	2.51
0.75	0.121	11.0	7.7	5.4	0.936	0.300	2.51
1.24	0.200	4.4	1.1	29.3	0.428	0.750	2.42
1.23	0.198	11.0	7.7	6.9	0.933	0.300	2.42
1.75	0.283	4.4	1.1	35.0	0.411	0.750	2.31
1.73	0.280	11.0	7.7	8.2	0.930	0.300	2.31
2.17	0.350	4.4	1.1	39.1	0.397	0.750	2.21
2.18	0.352	11.0	7.7	9.2	0.928	0.300	2.21
2.50	0.403	4.4	1.1	42.1	0.386	0.750	2.14
2.52	0.407	11.0	7.7	9.9	0.926	0.300	2.13
3.09	0.499	4.4	1.1	47.1	0.368	0.750	2.00
3.11	0.503	11.0	7.7	11.0	0.923	0.300	1.99
3.75	0.605	4.4	1.1	52.2	0.348	0.750	1.82
3.70	0.598	11.0	7.7	12.0	0.920	0.300	1.84

TABLE II: Upper (along the line of $E = 8.8, y = 0.75$) and lower (along the line of $E = 4.4, y = 0.75$) kinematics to measure the nuclear dependence of R.

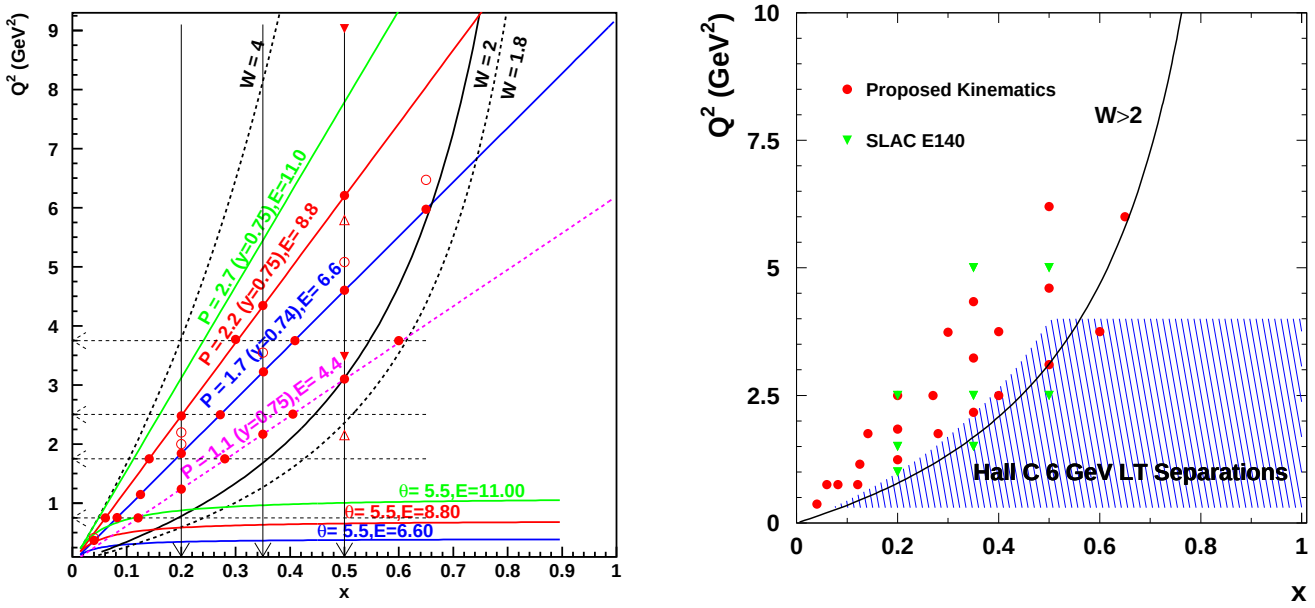

FIG. 8: The proposed kinematics with SHMS/HMS spectrometer with 4.4, 6.6,8.8 and 11.0 GeV beam, as well as the SLAC E140 and 6 GeV coverage on the right. The solid circles are the production kinematics to measure R with all proposed nuclear targets (H, D, C, Cu, Sn, Au), while the open circles and triangles are the test kinematics with only three targets (D, C, Au). Aluminum "Dummy" targets will be used for all kinematics for the end-cap subtraction for the deuterium targets.

$O(Q^2)$ vanishes when $Q^2 \to 0$ at fixed ν.

Thus we expect $R \to 0$ at the real photon limit of $Q^2 \to 0$ at fixed ν. This trend was not observed in the Hall C measurement with 6 GeV beam at fixed x, as seen in Figure 9 [3]. However, if we study the Q^2 distribution at fixed ν instead of fixed x, we may see a different Q^2 dependence. Fixed ν is equivalent to fixed W^2 at the limit of $Q^2 \to 0$.

3.3. Some Discussions on F_L

With the proposed data, one can also extract the longitudinal structure function F_L from the measured σ_L in the Rosenbluth technique, which can be directly related to the gluon distributions. It is not the primary goal of this proposal, but we will include the proposed data into the global fit and see how much the new data can help us to constrain the gluon

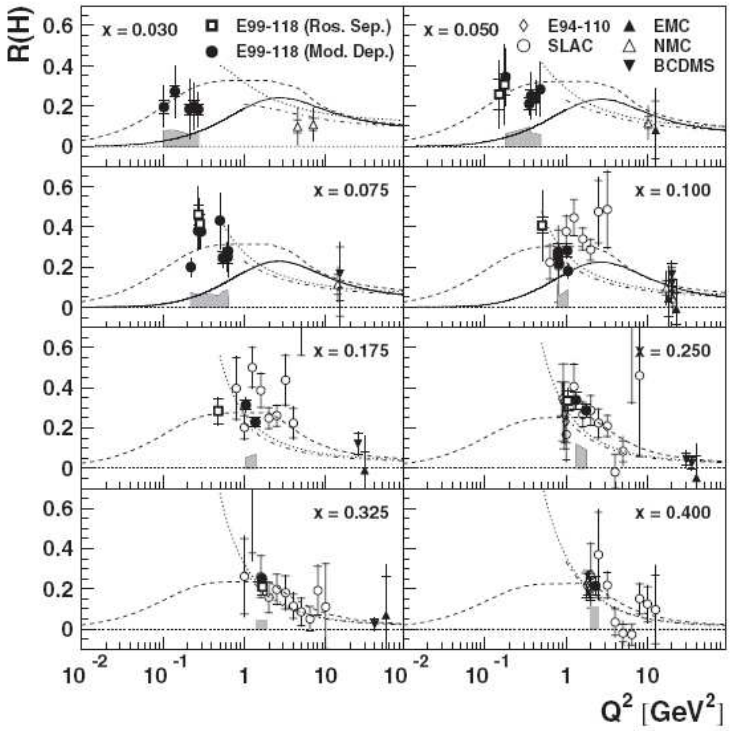

FIG. 9: [3] $R(x, Q^2)$ for hydrogen from JLab E99-118 experiment and other world measurements. The model dependent extraction of R (solid circles) is not as reliable as that with Rosenbluth technique (open squares). The dashed curve represents the JLab E99-118 parametrization, which assumes the form of $R_H = A(x)(1 - e^{-bQ^2})$ for $Q^2 < 2$ and connects to the SLAC Whitlow parametrization R_{1990} for $Q^2 > 2$. The fitted parameter $b = 9.212$ GeV^{-2}. The solid curves represent the model developed by Badelek, Kwiecinski and Staśto [23], based on the photon-gluon fusion mechanism. The dot-dashed curves are a next-to-next-to-leading order calculation based on MRST04 PDFs. The dotted curves show the next-to-leading order result of the GRV95 PDFs.

distributions as well as other PDFs in the nucleon and nuclei.

In the naive parton model, $F_L = 0$ for spin-1/2 quarks, giving the Callan-Gross relation $F_2 = 2xF_1$. However, the F_L structure function is non-zero at next-to-leading order (NLO), when the final state consists of qg, as may happen when the scattered quark radiates a gluon, or when the incoming quark has non-zero transverse momentum as can happen when the interacting quark comes from a gluon splitting. Hence, at NLO, F_L is given by a convolution involving the quark singlet (contribution from $q \to qg$) and the gluon density (contribution from $g \to q\bar{q}$) [19].

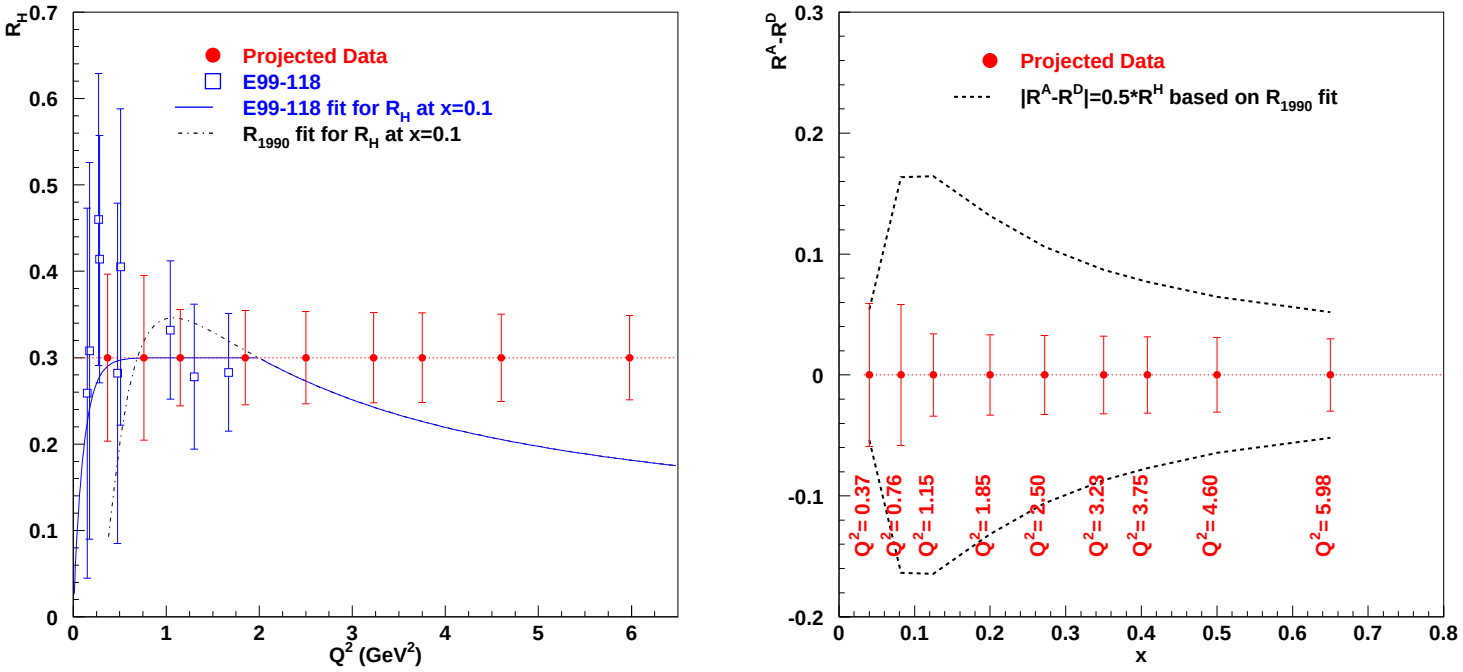

FIG. 10: [Left] Projected uncertainties for Q^2 dependence of R_H for central kinematics at fixed ν, which are estimated based on 1.8% relative uncertainty in point-point cross sections. The E99-118 data were estimated from the R and F_2 in Tvaskis's thesis. [Right] The projected uncertainties for the x dependence of $R_A - R_D$ for central kinematics, which are estimated based on 1.1% relative uncertainty in nuclear cross sections ratios.

While the quark densities in the region $0.05 < x < 0.6$ have been extensively studied in fixed target experiments and will be further explored with JLab 12 GeV, the behavior of the gluon density in this region is essentially unknown - especially in nuclei. The proposed measurements isolating the nuclear longitudinal structure function, F_L^A, may therefore provide unique access to nuclear gluons. Recent work has shown that nuclear effects on the longitudinal structure function closely follow those on the gluon distribution [20]. Probing gluons through F_L^A may provide new data to investigate gluon-specific nuclear effects.

The direct connection between F_L and gluon at NLO order can be explicitly shown for example in the "gluon" sum rule [21]:

$$F_L^{[n]}(Q^2) = \frac{\alpha_s(Q^2)}{\pi}\left[\frac{4}{3(n+1)}F_2^{[n]}(Q^2) + \frac{2c}{(n+1)(n+2)}(xG)^{[n]}(Q^2)\right] \qquad (12)$$

where $G(x)$ is the gluon density and $c = \sum_f e_f^2 = 2/3, 10/9, 11/9$ for number of quark flavors $N_f = 3, 4, 5$ respectively. The nth moment of the structure function $F(x, Q^2)$ is an integral over x, i.e. $F^{[n]}(Q^2) = \int_0^1 dx x^{n-2} F(x, Q^2)$. With inverse Mellin transform, the above equation can be changed into:

$$F_L(x, Q^2) = \frac{\alpha_s(Q^2)}{\pi} \left[\frac{4}{3} \int_x^1 \frac{dy}{y} (\frac{x}{y})^2 F_2(y, Q^2) + 2c \int_x^1 \frac{dy}{y} (\frac{x}{y})^2 (1 - \frac{x}{y}) y G(y, Q^2) \right] \quad (13)$$

Particularly for $n = 2$ and $N_f = 3$, Equation 12 becomes

$$\int_0^1 dx\ F_L(x, Q^2) = \frac{\alpha_s(Q^2)}{9\pi} \left[4 \int_0^1 dx\ F_2(x, Q^2) + \int_0^1 dx\ x\ G(x, Q^2) \right] \quad (14)$$

This sum rule has been checked with CTEQ and MSTW PDFs. It was found to work well in the lowest order of none-zero F_L with a careful treatment of heavy quark contributions.

To measure the moments accurately, a range of x data must be obtained at fixed Q^2 to determine the integral shape and size. It also needs to cover the resonance region at large x and DIS region at small x. JLab E94-110 has some precision data on F_L in the resonance region at Q^2=0.75,1.75,2.5,3.75 GeV^2 [2]. In the DIS region, the existing data mainly came from SLAC, in a global re-analysis of existing data from different experiments, and the uncertainties can be improved in this dedicated experiment.

There may, however, be sizable higher-twist effects in the proposed kinematics region, which can render parton distribution function extractions difficult and uncertain. The proposed L/T separated measurements covering a wide kinematics range will provide some constraint of the higher-twist effects.

4. EXPERIMENT

4.1. Experimental Overview

This experiment will use the standard HMS and SHMS spectrometers for inclusive measurements of scattered electrons from the A(e, e')X reaction. Measurements will be performed on hydrogen, deuterium, and solid targets including C, Cu, Sn and Au. The production rates are very high for most of our kinematics, therefore 4cm cryogenic targets and thin solid targets (1% radiation length except 2% for Au) will be used.

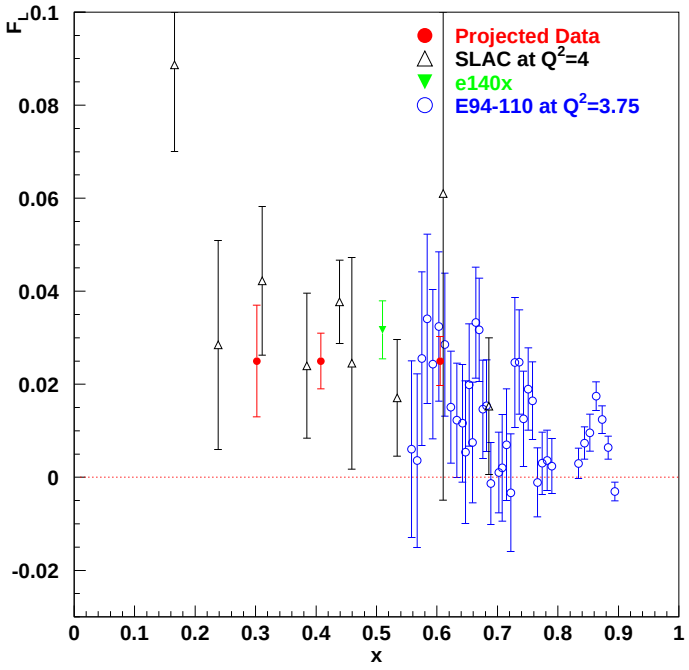

FIG. 11: The projected F_L structure function as a function of Bjorken x at $Q^2 = 3.75$ GeV^2, as well as the existing world data. The uncertainties are estimated assuming 1.5% relative uncertainty in cross section ratios with Whitlow's parameterization for R values(R_{1990}). Since the projected uncertainties are dominated by systematics, the projected data can be split into several finer-binned points without sacrificing the total uncertainties.

4.2. Systematic Uncertainty

The systematic uncertainty is the dominant source for all our kinematics, similar to the case of the Hall C 6 GeV program. For the R measurement, the normalization uncertainty cancels and we are only concerned about the point-point uncertainties. Referring to JLab E94-110 [24] and E99-118 [3] experiments, the systematic uncertainties are estimated in Table III. The total systematic uncertainty in the differential cross section is taken as the sum in quadrature of all systematic errors of the quantities that make up the cross section. Some detailed systematic studies can also be found in the Appendix.

Quantity	Uncertainty	$d\sigma_{DIS}/\sigma_{DIS}$ pt-pt
Beam Energy	0.04%	0.1%
Beam Charge	0.2 μ A	0.5 (*40/I)%
Scattered Electron Energy	0.04%	<0.1 %
Electronic Dead Time	0.25%	0.25%
Computer Dead Time	0.2%	0.2%
Tracking Efficiency	0.3%	0.3%
Detector Efficiency	0.2%	0.2%
Charge Symmetric Background	0.4%	0.4%
Acceptance	0.6%	0.6%
Scattered Electron Angle	0.5 mr	1.0 (*5.5/θ) %
Cryogenic Target Density	0.1%	0.1%
Cryogenic Target length	0.1%	0.1%
Cryogenic Target Background	0.3%	0.3%
Radiative Correction	1%	1% [a]
Total in Cryogenic Rosenbluth Separation	1.8%(1.5% at $\theta > 11.0$)	
Total in Nuclear Rosenbluth Separation	1.7%	
Total in Nuclear/Cryogenic Ratio	1.1%	

[a]It can be bigger for some kinematics.

TABLE III: Point-to-Point systematic uncertainties in the DIS cross section due to the uncertainty in various experimental quantities.

4.3. Beam Time Request

The beam energies we propose are **4.4, 6.6, 8.8 and 11 GeV**. The 4.4 GeV beam will be important to normalize the new 12 GeV data with the old 6 GeV data.

The targets we propose are **hydrogen, deuterium, ^{12}C, ^{63}Cu, ^{124}Sn and ^{197}Au** to have a wide coverage of A. An aluminum Dummy target will be also used for the subtraction of the target end-cap contributions. The Au target, also used in the SLAC E140 experiment [10], will maximize the Z-dependent or A-dependent effects, which is very important for the study

of $R_A - R_D$ as well as the Coulomb corrections. All the targets except tin have been proposed by other Hall C 12 GeV experiments. Our production rates are generally high so that we will use 4 cm cryogenic targets and 1% radiation length solid targets, except that we will use 2% gold target. Additionally, we will use Cu targets of different radiation lengths in order to check the corrections for external bremsstrahlung, for example the 2% and 6% length as proposed by E12-10-008 [25].

As with previous inclusive L/T separations, the proposed measurements will generally be dominated by systematic uncertainties. In fact, the L/T experiments during the 6 GeV program provided much of the studies which set the standards for both reducing and understanding the systematic uncertainties for the HMS spectrometer. It will be crucial to perform this same service for the SHMS. To do so will require a complete set of optics calibration data. The momentum scan and angle scan with overlapping acceptance but different central setting will be important for understanding the kinematic dependence of the acceptance and will be necessary for an analysis with finer binning. As with the 6 GeV program, these studies will benefit many Hall-C experiments in the future.

Only one spectrometer is required for each kinematics. The other spectrometer will be used to monitor the charge symmetric (or positron) backgrounds and the luminosity to control systematic uncertainties. To reduce the pt-pt systematics associated with beam current, target boiling, we plan to use a single beam current of 40 μA for all kinematics to measure R. However, we will use the current of 60 μA for the Coulomb scan, which has significantly lower rates. In addition we plan to perform several beam current calibrations, as well as target boiling studies at both high and low rate kinematics. The latter will allow a separation of a possible rate dependent systematic from true target boiling effects.

The beam time request is summarized in Table IV. This includes many kinematic settings and target changes. We have assumed an average overhead of 6 minutes for each angle/target change, 24 minutes for each momentum change, and 4 hours for each beam energy change based on the experience with 6 GeV program. The total requested beam time is 400.2 hours (17 days).

Category	Activity	Beam Time (Hours)
Production	R Measurements on H, D, Al, C, Cu, Sn, Au	158.1
(incl. Dummy)	Coulomb Scan at fixed ϵ on D,Al,C,Au	22.0
	Radiative Corrections Studies on D, Al, C, Au	37.0
Calibration	Detector Checkout	24.0
	Optics (Sieve/Open Collimator; P/θ scan)	24.0
	Elastic Scattering on H	24.0
	Beam Energy Measurements (4)	8.0
	Beam Current Calibration	8.0
	Horizontal Beam Position Scan on H/D	2.0
	Target Boiling/Rates Studies	16.0
	Charge Symmetry (Positron) Data (E=4.4)	16.0
Others	Beam Pass Changes (3)	12.0
	Target Changes (394)	39.4
	Angle Changes (61)	6.1
	Momentum Changes (9)	3.6
Total		400.2 (17 days)

TABLE IV: Beam time request assuming 100% efficiency.

5. SUMMARY

We propose to measure the nuclear dependence of R using several different targets (H, D, C, Al, Cu, Au), in the wide kinematics region $0.4 < Q^2 < 6$ GeV^2 and $0.04 < x < 0.65$, with the standard equipment in Hall C after the 12 GeV upgrade. We will study the nuclear dependence of R, disentangling the x and Q^2 dependence. In addition, we will also study the Q^2 dependence of R at fixed electron momentum and nuclear dependence of F_L.

6. COMMITMENT TO THE HALL C 12 GEV UPGRADE

The collaboration has a strong commitment to support the equipment for Hall C at 12 GeV.

Hampton University played a leading role in the 6 GeV L/T experiments at Hall C, which required many precision systematic studies. These studies led to the detailed understandings of the HMS spectrometer and benefited the Hall C program as a whole. These studies should be repeated for the SHMS spectrometer.

Hampton University is also responsible for leading the construction of the drift chambers for the SHMS spectrometer. The design of the drift chambers is complete and construction is starting this summer (2011). Progress is reported regularly to the SHMS collaboration. Further commitments include the installation of the chambers into the detector hut and commissioning.

As Hall C staff, David Gaskell will support the SHMS construction and detector assembly and is responsible for ensuring functionality of the Hall C Møller and Compton polarimeters at 12 GeV. He will also update and maintain the Hall C simulation package SIMC, which will help with the spectrometer optics calculations.

As Hall C staff, Patricia Solvignon will support Hall C experiments and participate in the SHMS construction. She will be in charge of the implementation of the Polarized ^{3}He target in Hall C.

APPENDIX A: EVENT RATES

The events rates were estimated assuming 40 μA current, 4 cm cryogenic and 1%(2% for Au) radiation length solid targets. The scattered electrons for most kinematics can be measured in both HMS or SHMS spectrometers, except that some momentum settings are less than the nominal SHMS momentum range of 2-11 GeV and some angular settings are smaller than the nominal HMS angular range of 10.5-85 degrees or bigger than the nominal SHMS angular range of 5.5-40 degrees. The momentum acceptance was assumed to be 16%, which is smaller than the full HMS/SHMS acceptance of $\pm$9%/(-10% to +22%). The angular acceptance was assumed to be 4 msr, which works for both HMS/SHMS too. The beam time was estimated based to achieve the 0.2% statistics (or 250k events) for deuterium target.

The production rates are high especially at low x or Q^2, therefore 0.3 hour is assumed for most kinematics. Ignoring the nuclear effects, the comparison of the rates for the solid target and that for deuterium can be estimated based on the ratios of their area densities:

$D : C(1\%) : Cu(1\%) : Sn(1\%) : Au(2\%) = 0.648 : 0.427 : 0.129 : 0.088 : 0.13 = 1 : 0.66 : 0.20 : 0.14 : 0.20$. The H:D ratio depends on the kinematics. It is about 1:2 at small x and 4:5 at $x = 0.65$ and $Q^2 = 6.0$ with 6.6 GeV beam. If running with the same beam time as deuterium, we will get 165k events (or 0.25% precision) for carbon, 50k events (or 0.45% precision) for copper/gold and 35k events (or 0.53%) for tin target.

APPENDIX B: STUDIES OF SYSTEMATIC UNCERTAINTIES

1. Radiative Corrections

Since the inelastic radiative corrections are not sensitive to the ϵ change and do not affect the extraction of R, we will be focusing on the quasi-elastic and elastic radiative corrections here, which are bigger at smaller y or the larger the ϵ. We have chosen y so that the quasi-elastic and elastic radiative corrections are less then 50% for all our kinematics, as shown in Figure 12. This means a 1% uncertainty in quasi-elastic and elastic cross section leads to <1% uncertainty in the Born cross section. The effect on R will be slightly smaller because of the partial cancellation between different ϵ points.

2. Coulomb Correction

The Coulomb corrections for the central kinematics to measure R are estimated based on the EMA approach, as shown in Figure 13. They are generally small except for the heavy targets at large Q^2, which corresponds to large x at fixed beam energy and scattered electron momentum. We will also take additional data to study the Coulomb correction procedure, as discussed in Section 3.1.

3. Charge Symmetric Background

Scattered electrons may come from π^0 decay instead of the deep-inelastic scattering on the quarks. This can be estimated using the SLAC Wiser fit of the pion production. The estimation is shown in Figure 14 for the central kinematics to measure R, assuming 0.7% RL material after the target. For fixed beam energy and scattered electron momentum,

Q^2	x_b	E	E'	θ	ϵ	y	W	Rate^D (Hz)	Time^D (h)
0.37	0.040	6.6	1.7	10.4	0.477	0.742	3.12	30k	0.3
0.36	0.040	8.8	3.9	5.9	0.737	0.557	3.12	282k	0.3
0.76	0.082	6.6	1.7	14.9	0.471	0.742	3.05	9.4k	0.3
0.75	0.082	8.8	3.9	8.5	0.734	0.557	3.05	84k	0.3
1.15	0.125	6.6	1.7	18.4	0.465	0.742	2.99	4.4k	0.3
1.15	0.125	8.8	3.9	10.5	0.730	0.557	2.99	39k	0.3
1.15	0.125	11.0	6.1	7.5	0.842	0.445	2.99	142k	0.3
1.85	0.201	6.6	1.7	23.4	0.454	0.742	2.87	1.67k	0.3
1.84	0.200	8.8	3.9	13.3	0.724	0.557	2.87	14.4k	0.3
1.84	0.200	11.0	6.1	9.5	0.838	0.445	2.87	51.8k	0.3
2.50	0.272	6.6	1.7	27.3	0.444	0.742	2.75	824.	0.3
2.50	0.271	8.8	3.9	15.5	0.718	0.557	2.75	6.9k	0.3
2.51	0.273	11.0	6.1	11.1	0.834	0.445	2.75	24.2k	0.3
3.23	0.351	6.6	1.7	31.1	0.433	0.742	2.62	412	0.3
3.21	0.349	8.8	3.9	17.6	0.711	0.557	2.62	3.4k	0.3
3.23	0.351	11.0	6.1	12.6	0.830	0.445	2.62	11.7k	0.3
3.75	0.408	6.6	1.7	33.6	0.426	0.742	2.52	256	0.3
3.75	0.407	8.8	3.9	19.0	0.706	0.557	2.52	2.11k	0.3
3.76	0.409	11.0	6.1	13.6	0.827	0.445	2.51	7.1k	0.3
4.59	0.499	6.6	1.7	37.3	0.413	0.742	2.34	120	0.6
4.60	0.500	8.8	3.9	21.1	0.699	0.557	2.34	930	0.3
4.57	0.497	11.0	6.1	15.0	0.822	0.445	2.35	3.2k	0.3
5.98	0.650	6.6	1.7	42.8	0.393	0.742	2.02	25.4	2.8
5.98	0.651	8.8	3.9	24.1	0.686	0.557	2.02	217	0.4
6.00	0.653	11.0	6.1	17.2	0.814	0.445	2.02	787	0.3

TABLE V: The event rates and beam time for the central kinematics (along the line of E=6.6,y=0.74) to measure the nuclear dependence of R. Rates are estimated assuming 40 μA beam current on a 4 cm deuterium cell. The beam times are calculated to get 250k deuterium events with the minimum to be 0.3 hour.

Q^2	x_b	E	E'	θ	ϵ	y	W	Rate^D (Hz)	Time^D (h)
0.75	0.061	8.8	2.2	11.3	0.464	0.750	3.54	15.6k	0.3
0.74	0.060	11.0	4.4	7.1	0.685	0.600	3.54	98.6k	0.3
1.75	0.141	8.8	2.2	17.3	0.455	0.750	3.39	3.23k	0.3
1.75	0.141	11.0	4.4	10.9	0.679	0.600	3.39	19.5k	0.3
2.50	0.202	8.8	2.2	20.7	0.449	0.750	3.28	1.52k	0.3
2.48	0.200	11.0	4.4	13.0	0.675	0.600	3.28	9.08k	0.3
3.74	0.302	8.8	2.2	25.4	0.438	0.750	3.09	565	0.3
3.75	0.303	11.0	4.4	16.0	0.667	0.600	3.08	3.23k	0.3
4.34	0.351	8.8	2.2	27.4	0.433	0.750	2.99	369	0.3
4.33	0.350	11.0	4.4	17.2	0.664	0.600	2.99	2.12k	0.3
6.21	0.501	8.8	2.2	32.9	0.417	0.750	2.66	102	0.7
6.19	0.500	11.0	4.4	20.6	0.653	0.600	2.66	582	0.3
0.75	0.121	4.4	1.1	22.7	0.444	0.750	2.51	3.98k	0.3
0.75	0.121	11.0	7.7	5.4	0.936	0.300	2.51	951k	0.3
1.24	0.200	4.4	1.1	29.3	0.428	0.750	2.42	1.49k	0.3
1.23	0.198	11.0	7.7	6.9	0.933	0.300	2.42	312k	0.3
1.75	0.283	4.4	1.1	35.0	0.411	0.750	2.31	678	0.3
1.73	0.280	11.0	7.7	8.2	0.930	0.300	2.31	120k	0.3
2.17	0.350	4.4	1.1	39.1	0.397	0.750	2.21	383	0.3
2.18	0.352	11.0	7.7	9.2	0.928	0.300	2.21	58.1k	0.3
2.50	0.403	4.4	1.1	42.1	0.386	0.750	2.14	235	0.3
2.52	0.407	11.0	7.7	9.9	0.926	0.300	2.13	34.9k	0.3
3.09	0.499	4.4	1.1	47.1	0.368	0.750	2.00	77.8	0.9
3.11	0.503	11.0	7.7	11.0	0.923	0.300	1.99	15.4k	0.3
3.75	0.605	4.4	1.1	52.2	0.348	0.750	1.82	14.3	4.9
3.70	0.598	11.0	7.7	12.0	0.920	0.300	1.84	7.10k	0.3

TABLE VI: The event rates and beam time for the upper and lower kinematics (along the line of E=6.6/8.8,y=0.75) to measure the nuclear dependence of R. Rates are estimated assuming 40 μA beam current on a 4 cm deuterium cell. The beam times are calculated to get 250k deuterium events with the minimum to be 0.3 hour.

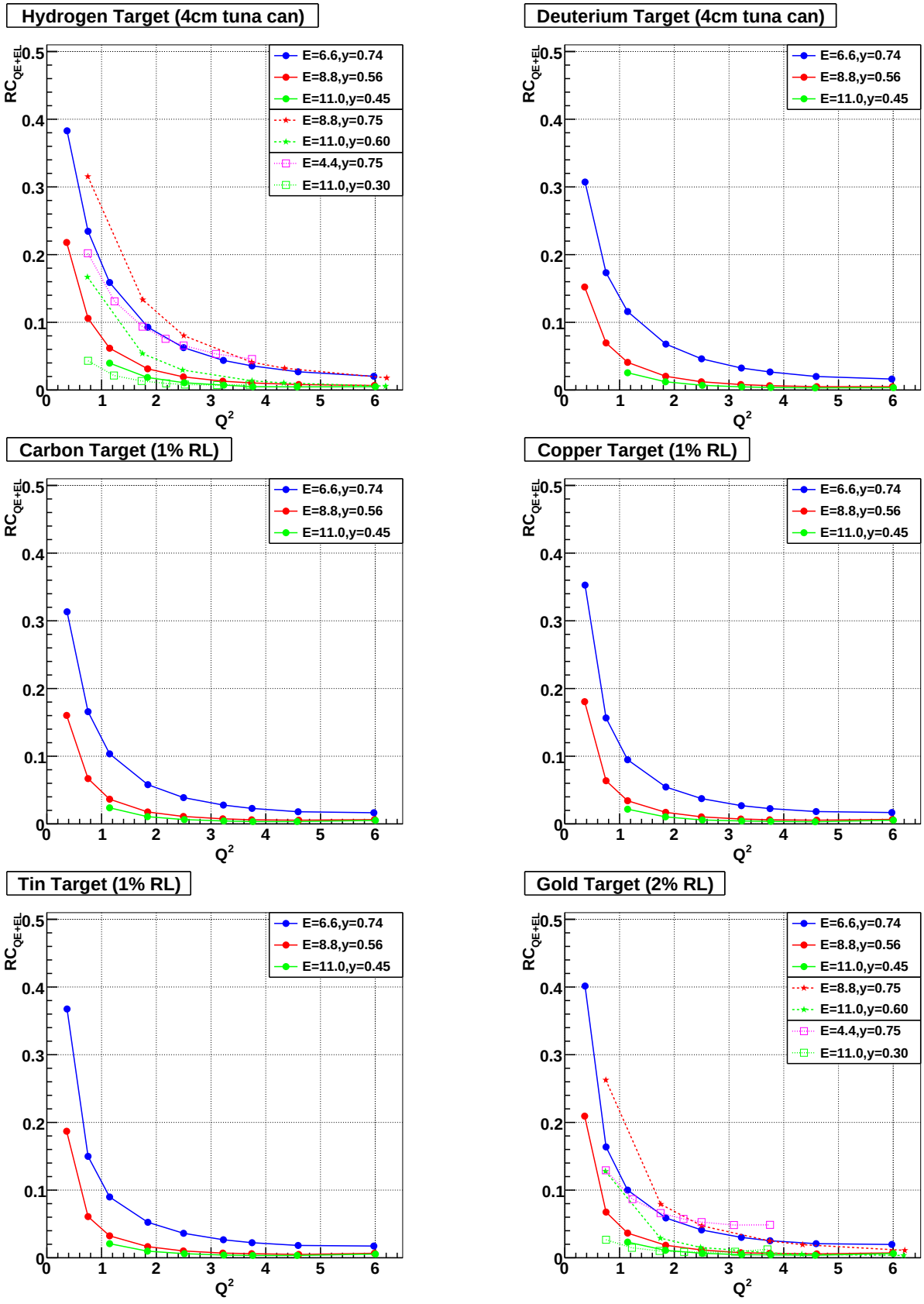

FIG. 12: The quasi-elastic and elastic radiative corrections, in terms of $RC_{QE+EL} = \frac{\sigma_{QE}+\sigma_{EL}}{\sigma_{QE}+\sigma_{EL}+\sigma_{Born}}$, for the central kinematics to measure R.

Q^2	x_b	E	E'	θ	ϵ	y	W	Rate^D (Hz)	Time^D (h)	Time^{Au} (h)
0.41	0.040	6.6	1.2	13.0	0.346	0.818	3.26	10.9k	0.3	0.3
0.41	0.040	8.8	3.4	6.7	0.669	0.614	3.26	148k	0.3	0.3
0.49	0.048	11.0	5.6	5.1	0.806	0.491	3.24	478k	0.3	0.3
2.03	0.200	6.6	1.2	29.3	0.322	0.818	3.00	590	0.3	0.3
2.04	0.201	8.8	3.4	15.0	0.653	0.614	3.00	7.61k	0.3	0.3
2.02	0.200	11.0	5.6	10.4	0.797	0.491	3.00	30.9k	0.3	0.3
2.21	0.200	6.6	0.7	40.5	0.180	0.894	3.12	146	0.3	0.5
2.23	0.201	8.8	2.9	17.0	0.574	0.670	3.12	4.00k	0.3	0.3
2.21	0.200	11.0	5.1	11.4	0.750	0.536	3.12	18.5k	0.3	0.3
3.55	0.350	6.6	1.2	39.1	0.301	0.818	2.73	80.1	0.4	0.9
3.57	0.353	8.8	3.4	19.9	0.639	0.614	2.73	1.79k	0.3	0.3
3.56	0.351	11.0	5.6	13.8	0.788	0.491	2.73	7.03k	0.3	0.3
5.08	0.501	6.6	1.2	47.2	0.280	0.818	2.44	41.5	0.7	1.7
5.09	0.502	8.8	3.4	23.8	0.626	0.614	2.43	501	0.3	0.3
5.07	0.501	11.0	5.6	16.5	0.779	0.491	2.44	1.92k	0.3	0.3
6.60	0.651	6.6	1.2	54.3	0.260	0.818	2.10	9.5	2.9	6.9
6.67	0.658	8.8	3.4	27.3	0.612	0.614	2.09	111	0.3	0.7
6.64	0.655	11.0	5.6	18.9	0.770	0.491	2.09	460	0.3	0.3

TABLE VII: The event rates and beam time for the kinematics to study radiative correction. Rates assume 40 μA on a 4 cm deuterium cell. The beam times are estimated to take 100k for deuterium events and 50 k for gold target, with the minimum to be 0.3 hour. We will take short run (0.3 h) with dummy target for deuterium background subtraction. The beam time for carbon will be the same as deuterium, which allows us to take 66k events.

the background is bigger at smaller angle or smaller x and Q^2. For fixed x and Q^2, the background is bigger at bigger y or smaller ϵ.

During the experiment, we will also measure the charge symmetric background by detecting the positrons. We will place SHMS and HMS on the two sides of the target, with the same momentum and angle settings, but with different polarities. The data will help us

Q^2	x_b	E	E'	θ	ϵ	y	W	C^{Au}_{Coulomb}	Rate^D (Hz)	Time^D (h)	Rate^A (Hz)	Time^A (h)
3.48	0.50	4.4	0.69	64.6	0.20	0.84	2.08	11.6%	23.9	1.2	4.1	3.4
9.03	0.50	11.0	1.38	45.5	0.20	0.88	3.10	6.2%	10.5	2.7	1.8	7.8
2.15	0.50	4.4	2.11	27.9	0.70	0.52	1.74	3.5%	1.31k	0.3	223	0.3
5.79	0.50	11.0	4.83	19.0	0.70	0.56	2.58	1.9%	662	0.3	114	0.3

TABLE VIII: The event rates, beam time as well as the Coulomb correction for the Coulomb scan test data. Rates assume 60 μA on a 4 cm deuterium cell and a 2% radiation length gold target. Times are for 100k (50k) events for deuterium (gold) at the $\epsilon = 0.2$ settings. We will take short run (0.3 h) with dummy target for deuterium background subtraction. The beam time for carbon will be the same as deuterium, which allows us to take 66k events.

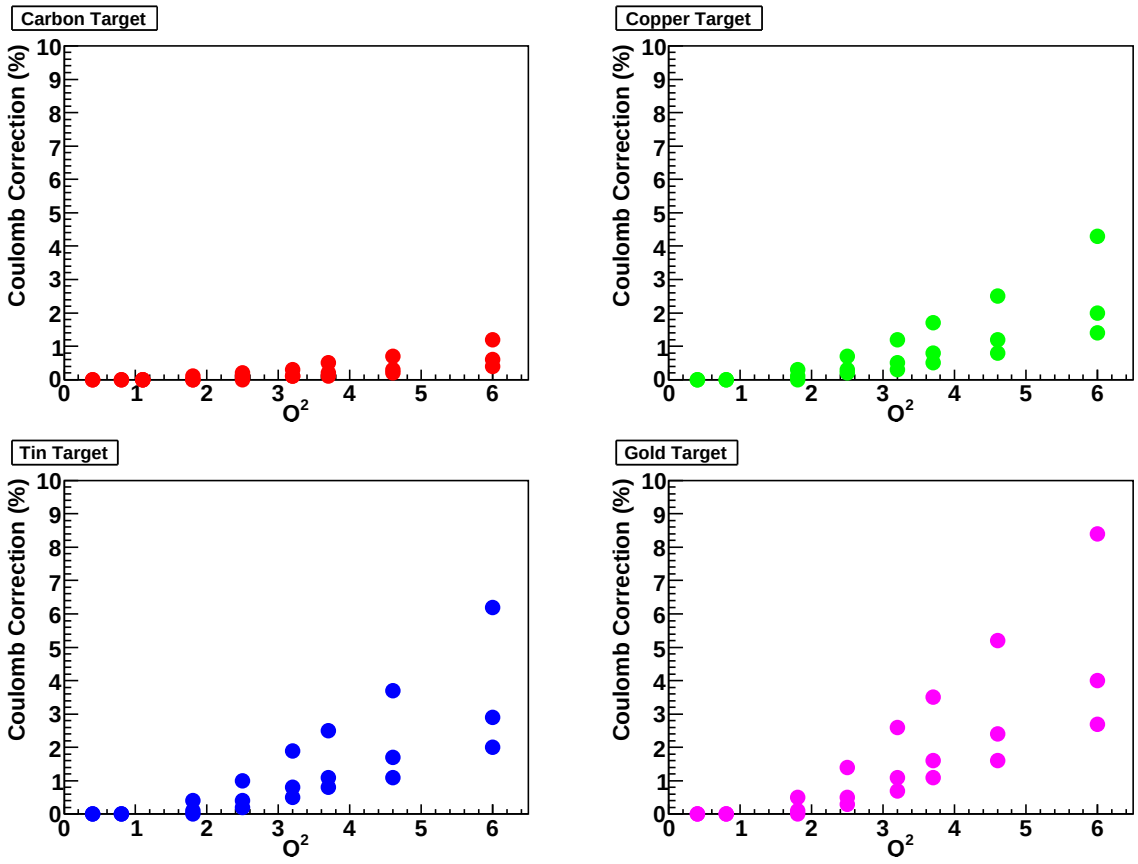

FIG. 13: The Coulomb corrections for the central kinematics to measure R. The corrections are estimated on the EMA approach.

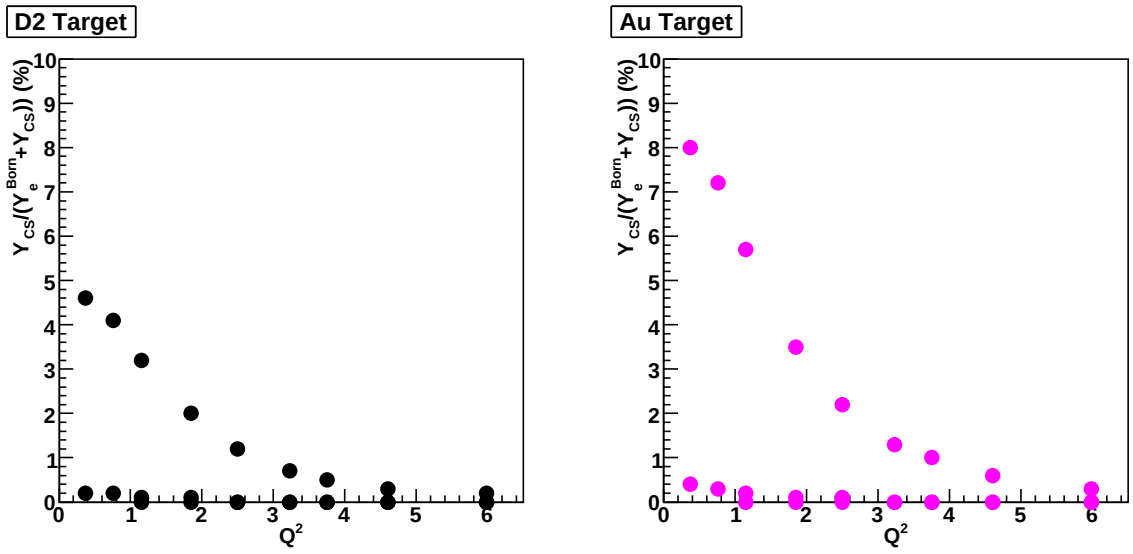

FIG. 14: The Charge Symmetric Corrections for the central kinematics to measure R. The corrections for H2 is slightly smaller than that of D2. The corrections for the other 1% solid targets (C, Cu, Sn) are between those for 4cm D2 and 2% Au target.

to refine the model calculations.

4. π^-/e Ratio

The π^-/e ratio was estimated for all the central kinematics, which is about 40:1 in the worst case. With the pion rejection factor of 10^{-4}, the contribution of the π^- background to the cross section is less than 0.4%. The subtraction of the charge symmetric background will further reduce the pion contributions.

---

[1] L. W. Whitlow *et al.*, Phys. Lett. B **250**, 193 (1990); L. W. Whitlow, Ph.D. Thesis, SLAC-REPROT-357, Standford University (1990).

[2] Y. Liang *et al.*, nuc-ex/0410027; E94-110 experiment, spokesperson: C.E. Keppel, *Measurement of $R = \sigma_L/\sigma_T$ in the Nucleon Resonance Region.*

[3] V. Tvaskis *et al.*, Phys. Rev. Lett. **98**, 142301 (2007) (nucl-ex/0611023); Vladas Tvaskis, Ph.D Thesis, *Longitudinal-Transverse Separation of Deep-Inelastic Scattering at low Q^2 on Nucleons and Nuclei*, Vrije Universiteit (2004); E99-118 experiment, spokespersons: A. Bruell,

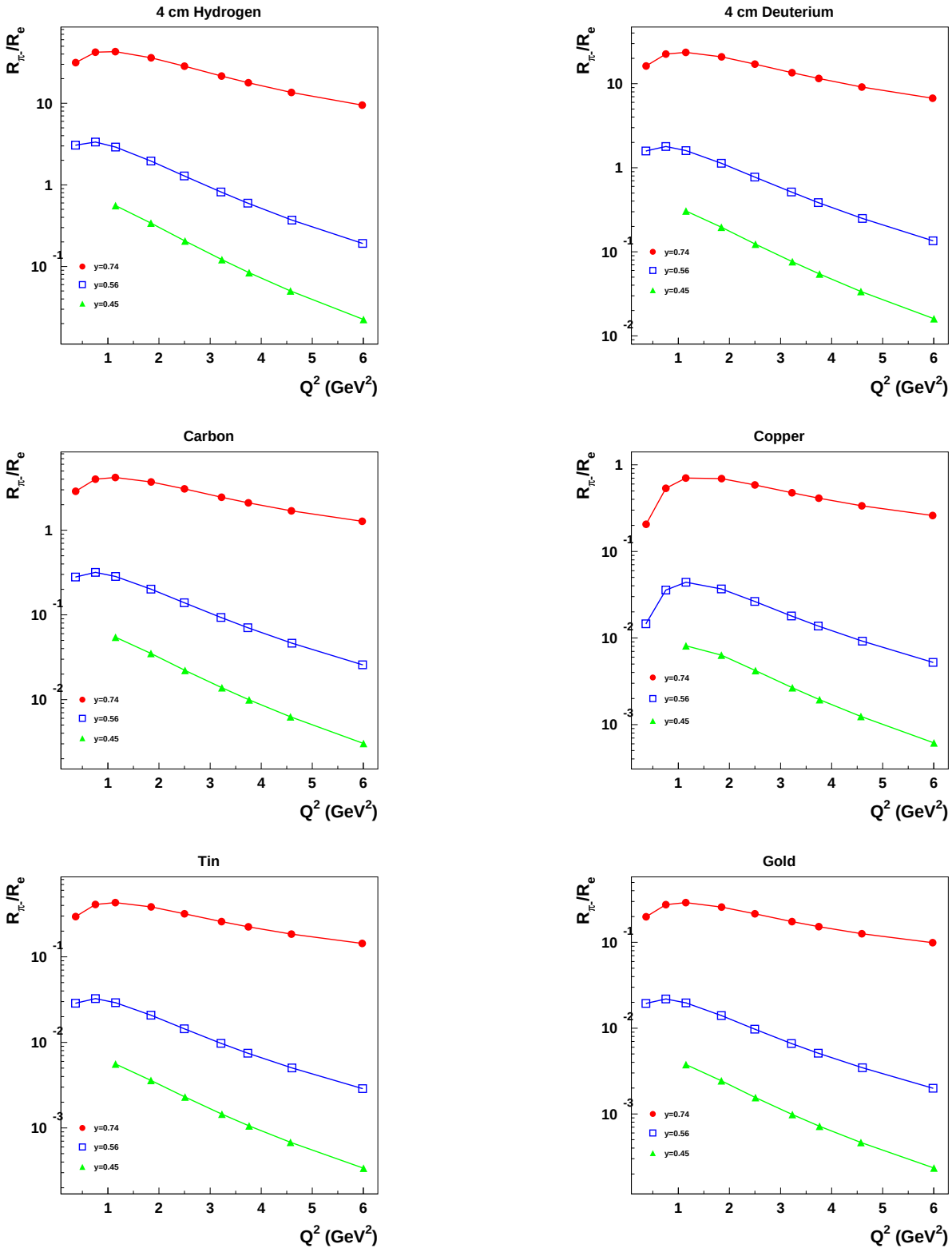

FIG. 15: The singles π^-/e ratio for the central kinematics to measure R.

ϵ	Q^2	Target	C_{RAD}	Y_π^-/Y_e	$Y_{CS}/(Y_e^{Born}+Y_{CS})$
0.2	3.48	D	1.17	161	0.108
0.2	9.03	D	1.11	106	0.043
0.2	3.48	Au	1.11	6.1	0.180
0.2	9.03	Au	1.09	1.8	0.076
0.7	2.15	D	0.96	6.2	0.0
0.7	5.79	D	0.94	0.6	0.0
0.7	2.15	Au	0.93	1.4	0.0
0.7	5.79	Au	0.91	0.2	0.0

TABLE IX: Backgrounds and radiative corrections factors for Coulomb correction scan settings. Dominant backgrounds are from pion contamination and charge symmetric processes. A 2% gold target has been chosen to minimize (external) radiative corrections and contributions from the charge summetric backgrounds.

J. Dunne, and C.E. Keppel, *Measurement of the Nuclear Dependence of $R = \sigma_L/\sigma_T$ at Low Q2*.

[4] E00-002 experiment, spokespersons: C.S. Armstrong and M. I. Niculescu, *F2N at Low Q2*.

[5] E02-109 experiment, spokespersons: M. E. Christy and C.E. Keppel, *Measurement of $R = \sigma_L/\sigma_T$ on Deuterium in the Nucleon Resonance Region*.

[6] E04-001 experiment, spokespersons: A. Bodek and C.E. Keppel, *Measurements of F2 and R on Nuclear Targets in Resonance Region*.

[7] E06-009 experiment, spokespersons: M. E. Christy and C.E. Keppel, *Measurement of $R = \sigma_L/\sigma_T$ on Deuterium in the Nucleon Resonance Region and Beyond*.

[8] M. N. Rosenbluth, Phys. Rev. **79**, 615 (1956).

[9] P. Solvignon, D. Gaskell and J. Arrington, AIP Conf. Proc. **1160**, 155 (2009) [arXiv:0906.0512 [nucl-ex]].

[10] S. Dasu *et al.*, Phys. Rev. D **49**, 5641 (1994).

[11] J. Seely *et al.*,Phys. Rev. Lett. **103**, 202301 (2009); E03-103 experiment, spokespersons: J. Arrington and D. Gaskell, *A Precise Measurement of the Nuclear Dependence of Structure Functions in Light Nuclei*.

[12] A. Aste, C. von Arx and D. Trautmann, Eur. Phys. J. A **26**, 167 (2005) [arXiv:nucl-th/0502074].

[13] A. W. Aste, Nucl. Phys. A **806**, 191 (2008) [arXiv:0710.1261 [nucl-th]].

[14] J. J. Aubert *et al.*, Phys. Lett. B **123**, 275 (1983).

[15] D. F. Geesaman, K. Saito, A. W. Thomas, Ann. Rev. Nucl. Part. Sci. **45**, 337-390 (1995).

[16] P. R. Norton, Rept. Prog. Phys. **66**, 1253-1297 (2003).

[17] J. Gomez, R. G. Arnold, P. E. Bosted, C. C. Chang, A. T. Katramatou, G. G. Petratos, A. A. Rahbar, S. E. Rock *et al.*, Phys. Rev. **D49**, 4348-4372 (1994).

[18] J. Ashman *et al.* [European Muon Collaboration], Phys. Lett. **B202**, 603 (1988).

[19] C. G. Callan and D. J. Gross, Phys. Rev. Lett. **22**, 156 (1969); G. Altarelli and G. Martinelli, Phys. Lett. **B76**, 89 (1978).

[20] N. Armesto, H. Paukkunen, C. A. Salgado and K. Tywoniuk, Phys. Lett. B **694**, 38 (2010).

[21] R. G. Roberts, *The structure of the proton: Deep Inelastic Scattering*, Cambridge University Press, p88,p95 (1990).

[22] K. Ackerstaff *et al.*[HERMES Collaboration], Phys. Lett. B **475**, 386 (2000) and erratum, Phys. Lett. B **567**, 339 (2003).

[23] B. Badelek, J. Kwiecinski, and A. Staśto, Z. Phys. **C74**, 297 (1997).

[24] M. E. Christy, Phys. Rev. C **70**, 015206 (2004).

[25] E12-10-008 experiment, spokespersons: J. Arrington, A. Daniel and D. Gaskell, *Detailed studies of the nuclear dependence of F_2 in light nuclei.*